

# Shear test of the off-axis surface with an axis-symmetric parent

Peng Su, James H. Burge, Jose Sasian

College of Optical Sciences, University of Arizona, Tucson, AZ 85721

## ABSTRACT

Interferometers with additional test optics are frequently used for measuring aspherical optical surfaces. In optical testing it is desirable to separate the figure measurement errors due to the test surface from figure errors that arise in the test equipment. For axially symmetric optics this is accomplished by rotating the surface being measured with respect to the test system. The data can then be processed to separate the non-axially symmetric errors that are fixed in the test system and those that rotate with the part. The axially symmetric errors cannot be distinguished with this technique. In this paper we present a variation of this technique for off-axis aspheric optics. The rotation is performed by rotating the test surface about the optical axis of its parent asphere, which may be outside the physical boundary of the test surface. As these rotations cannot be large, this motion is better described as a shear of the optical surface with respect to the test optics. By taking multiple measurements with different amounts of rotational shear and using maximum likelihood estimation methods, one can separate the errors in the test optics from the irregularity in the optical surface.

Keywords: Telescopes, interferometry, optical testing, optical fabrication, aspheres

## 1. INTRODUCTION

The symmetry of a mirror segment with respect to rotation about its parent's optical axis can be exploited to verify the accuracy of the optical test in important respects. An ideal off-axis segment can be rotated about its parent axis and the apparent shape of the mirror will not change. This geometry is shown in Figure 1. The interferometer views the mirror in fixed coordinates that do not rotate with the segment, so any changes in the apparent shape are due to figure errors that are not symmetric about this axis. This change is independent of errors in the test system. This technique is a variation of a common method that is used for axially symmetric surfaces [1, 2].

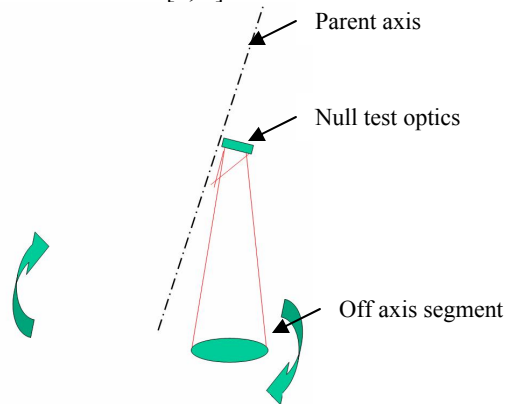


Fig. 1. Basic concept of the shear test

We designed a shear test to verify the off-axis parabolic primary mirror of the New Solar Telescope (NST). The shear in this test was realized by rotating the mirror around its parent axis and taking interferograms at difference shearing positions, while the null test optics was unchanged during the shearing. This shear test allowed one to separate the errors that move with the mirror from the errors that stay in the null test optics. The Singular Value Decomposition (SVD)[3] method was used to perform a least squares estimate of both mirror and null optics. The setting of the estimate threshold was based on the Wiener filter concept and a Monte Carlo analysis. Test errors with rotational symmetry about the parent axis, errors with periodicity that repeat as the shear angles, and errors that could not be determined because the

low orders terms were not included, were systematically determined from a numerical analysis. The outputs of the shearing test were separated into four parts, errors in the test surface, errors in the null system, terms in the null space, which could come from either the mirror or the null test and noise.

## 2. DATA REDUCTION

### 2.1 System matrix

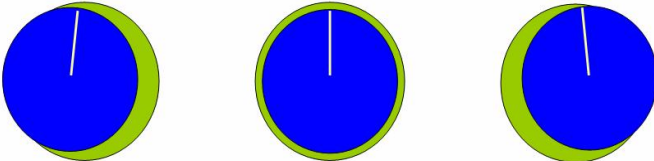


Fig. 2. Configuration of the NST shear test

The mirror was rotated clock wise and counter-clock wise about its parent axis by approximately 3°, and three sets of interferograms were taken at each position. Based on our data reduction experience in a previous test for a flat mirror [4], we applied the Maximum likelihood estimate (MLE) method to this application. For this discussion we call the mirror and the null optics A and B respectively and the optical figure of both is described by Zernike polynomials. Three sets of basis functions were generated by the SVD method to span the effective data regions of the three measurements. Data in each measurement after fitted by the basis function were represented by the fitting coefficients, which formed a data column vector  $y$ . A system matrix  $M$  was created to related the polynomial coefficients of A and B to the phase vector  $y$ . The shear test was described as

$$y = M * x \tag{1}$$

where  $x$  is a vector containing the coefficients to be estimated.

$$x = [\text{coefficients of surface A, coefficients of surface B, alignment coefficients}] \tag{2}$$

and  $M$  is the system matrix determined by the test geometry as shown in Fig.3.

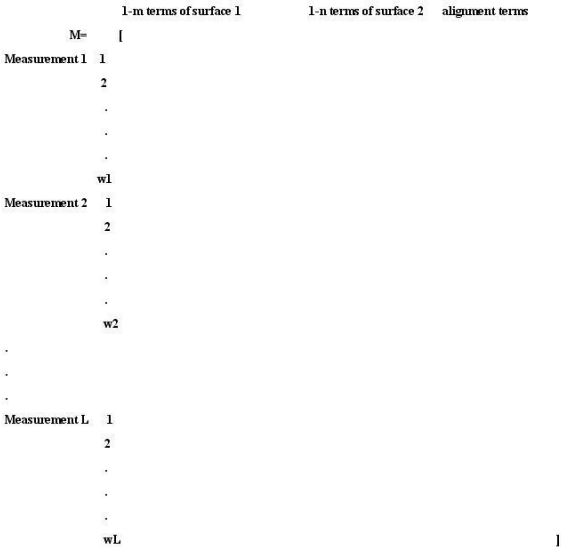


Fig. 3. The structure of the system matrix M

where  $m$  and  $n$  are the numbers of polynomials used to describe surface A and B.  $w_1, w_2 \dots w_L$  are the numbers of the polynomials being used as the basis for each measurement. The matrix described the effect caused by each surface polynomial term or the alignment terms to the basis functions in each measurement. For example  $M_{32}$  described the effect of the second polynomial of surface A to the third function in the basis one. Detailed description of system matrix  $M$  can also be found in reference [4]. Because each measurement has different amount of piston, tilt, power, etc, due to the alignment, extra alignment terms were added in the vector  $x$ , and corresponding columns were also added in the matrix  $M$ . This made it possible to have different fitting coefficients of the alignment terms for each measurement. After setting the system matrix and obtaining the phase vector  $y$ , our task was to estimate coefficient vector  $x$ .

## 2.2 Test null space

From physical insight, we know that certain kinds of errors cannot be separated from the test surface and the test optics by a simple shear motion. For instance, these errors may include errors with rotational symmetry around the parent axis, errors with periodicity that repeat as the shear angles, and shape error terms related with the alignment errors (for instance, piston, tilt, power and certain combinations of the astigmatism and coma). These errors constitute the null space of this shear test, and can be numerically derived from the system matrix as shown next.

To determine the null space, the SVD method is used to decompose the system matrix  $M$ . SVD can be thought as a generalized spectrum analysis of the rectangular matrix.  $M$  can be uniquely be decomposed as:

$$M=U*S*V' \tag{3}$$

Where  $U$  is a unit matrix that describes the range of the shear test and  $S$  is the singular value matrix. The diagonal components are the singular values of the matrix  $M$ , which reflect the noise sensitivity of the surface error modes under estimation.  $V$  is also a unit matrix, it describes the domain or the solution space of the test. The columns in  $V$  which correspond to zero singular values in  $S$  are the null space of the matrix.

## 2.3 Generating null space vectors numerically

Errors in the null space can not be separated between A and B, so the solution vectors formed by certain combinations of them satisfy the requirement for the null space of the system matrix ( $M*x=0$ ). Vice versa, the null space vectors calculated from SVD imply that certain errors in A will cancel certain errors in B, which means that these errors that are not separable are the null space of the test. So the null space of the matrix is the null space of the test.

Based on above argument, we can obtain the null space of the test directly from the matrix  $V$ , which is generated by SVD. The figures in Fig. 4 show the null space of the shear test with 37 Zernike terms used to describe each surface without including the alignment terms in the system matrix. They are rotational symmetric errors.

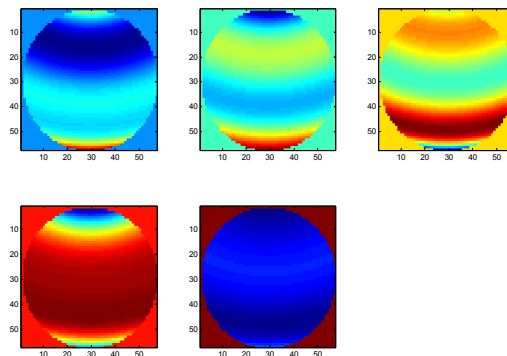


Fig. 4. Null space without considering alignment terms

## 2.4 Separating out the null space from surface estimates

Errors in the null space are not separable between test surface and test optics. When MLE is performed to estimate the surfaces, these errors fall into the two surface estimates based on the minimal norm criteria. So the estimate results need to be further processed to separate the null space out of the surface estimates. This can be realized by least square fitting the surface estimate results with null space vectors generated by SVD and then removing the fitting data from the surface estimates.

As an example of removing the null space consider the following. 100 nm coma as shown in Fig.5 (a) is used as an input of surface A, and no error is put in surface B. After removing the null space, 71nm of the surface information is left as shown in Fig.5 (b), which can be estimated accurately without noise being present. In Fig.5 (c), the blue lines represent the input Zernike coefficients in surface A and B, while red lines are the estimate results which are buried by the null space errors. Fig.5 (d) shows that we can estimate the remaining information accurately after removing the null space.

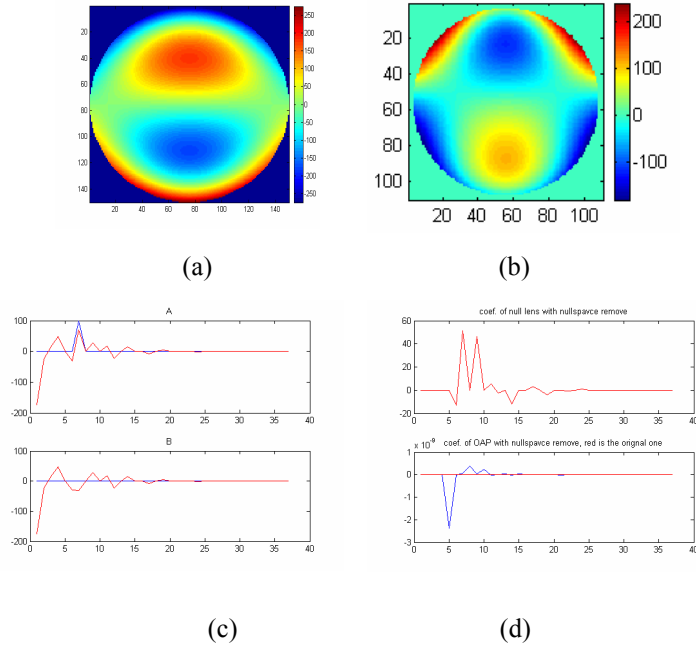


Fig. 5. Separating out the null space errors

## 2.5 Solution space and noise sensitivity

Using SVD, the estimate of the solution vector  $x$  can be expressed as:

$$x = \sum_{i=1}^n \frac{y \cdot U_i'}{\omega_i} V_i \quad (4)$$

where  $y$  is the phase data vector,  $U_i$  is the  $i$ th column of matrix  $U$ ,  $\omega_i$  is the  $i$ th singular value in matrix  $S$ , and  $V_i$  is the  $i$ th column of matrix  $V$ .  $V_i$  can be thought as a certain combination of errors in A and B. This combination is a certain mode to be estimate. Errors in A and B to be estimated from the test can be decomposed as the combinations of columns in  $V$ . Singular values  $\omega_i$  tell us that with one unit of a mode in  $V$ , how many units of signals will be generated, which is  $U_i$ . The larger the singular value of a certain mode, the bigger the signal will be generated during the shear test and the

better the noise insensitivity it has. Thus the above equation means that first we project the phase data to the range vectors, and then we divide them by the singular value. The result will be the magnitude of certain mode in the surfaces. The estimate is a combination of different modes. Robustness of the modes is determined by the signal magnitude generated by one unit of the mode, which is the corresponding singular value of that mode. Rather than stating that a certain term in A or B is insensitive to the noise, we can state that certain combination of the errors can be well estimated.

### 2.6 Threshold estimate

A given mode with a small singular value will amplify the noise greatly as modes are divided by a small value. So in the presence of noise and keeping all the modes, the estimate coefficients or surface errors can become extreme large due to noise coupling. Using the concept of Winner filter, we derived the coefficients used to multiplying each mode in the above equation to give a best least square estimate under the existence of noise.

Assume Gaussian noise existing in the measurements, the best least square estimate of the surfaces under the existence of noise is given as following:

$$x = \sum_{i=1}^n \frac{y.U_i'}{\omega_i} V_i * \phi_i \tag{5}$$

$$\phi_i = \frac{y.U_i'.y.V_i'}{y.U_i'.y.V_i'+N.U_i'.N.V_i'} \tag{6}$$

where N is an estimate of the phase noise vector. From the equation we see that when signals are dominant, the factor  $\phi_i$  becomes equal to one and when the noise is dominant, the factor becomes equal to zero.

### 2.7 Examples to show the ability to estimate and noise sensitivities

To simplify the procedure and without losing the significance, zero and one are used as the values for factors  $\phi_i$ . It means that a threshold is selected to discard the modes corresponding to small singular values. Table 1 describes the estimate ability of Zernike terms 5-16, considering the null space removal and noise sensitivity issue. With certain noise level in our experimental data, a threshold of 10 was being used here. The table shows that for lower order aberrations, astigmatism, coma, and trefoil could not be well estimated. However, the table shows that the shear test is very good at detecting higher order aberrations.

**Table 1. Ability to estimate Zernike terms 5-16**

Zernike terms (A=10 B=10)	Z5	Z6	Z7	Z8
Estimate with threshold =0	rmsa =10 rmsb= 10 rmserrora =0 rmserrorb=0	rmsa = 1.8 rmsb= 1.8 rmserrora =0 rmserrorb=0	rmsa = 7.1 rmsb= 7.1 rmserrora =0 rmserrorb=0	rmsa =10 rmsb =10 rmserrora=0 rmserrorb=0
Estimate with threshold =10	rmsa = 0.9 rmsb = 0.9 rmserrora = 9.1 rmserrorb = 9.1	rmsa = 1.8 rmsb = 1.8 rmserrora = 1 rmserrorb= 1	rmsa = 7.1 rmsb = 7.1 rmserrora= 0.3 rmserrorb= 0.3	rmsa = 6.9 rmsb = 6.9 rmserrora=3.2 rmserrorb=3.2

Zernike terms (A=10 B=10)	Z9	Z10	Z11	Z12
Estimate with threshold =0	rmsa =7 rmsb= 7 rmserrora =0 rmserrorb=0	rmsa =10 rmsb= 10 rmserrora =0 rmserrorb=0	msa =9.1 rmsb= 9.1 rmserrora =0 rmserrorb=0	msa =8 rmsb= 8 rmserrora =0 rmserrorb=0
Estimate with threshold =10	rmsa = 7 rmsb= 7 rmserrora =0.2 rmserrorb=0.2	rmsa = 5.7 rmsb = 5.7 rmserrora=4.5 rmserrorb=4.5	rmsa = 8.9 rmsb = 8.9 rmserrora=0.9 rmserrorb=0.9	rmsa = 7.8 rmsb = 7.8 rmserrora=1 rmserrorb=1
Zernike terms (A=10 B=10)	Z13	Z14	Z15	Z16
Estimate with threshold =0	rmsa = 10 rmsb= 10 rmserrora =0 rmserrorb=0	rmsa = 7.7 rmsb= 7.7 rmserrora =0 rmserrorb=0	msa = 10 rmsb= 10 rmserrora =0 rmserrorb=0	msa = 10 rmsb= 10 rmserrora =0 rmserrorb=0
Estimate with threshold =10	rmsa =9.9 rmsb = 9.9 rmserrora = 0.6 rmserrorb = 0.6	rmsa =7.7 rmsb = 7.7 rmserrora =0.5 rmserrorb =0.5	rmsa =9.7 rmsb=9.7 rmserrora= 1.2 rmserrorb=1.2	rmsa =10 rmsb =10 rmserrora = 0 rmserrorb =0

where rmsa and rmsb are the rms values of the surface A and B, rmserrora and rmserrorb are the estimate errors of them.

### 3. EXPERIMENTAL RESULTS

A shear test was performed to measure the NST mirror. The mirror was rotated clock and counter clock-wise by approximately 3 degrees around its parent axis. Three sets of the interferograms were taken.

### 3.1 Estimate surfaces with lower order aberration removed

Because there are relative large uncertainties of in the measurement of lower order aberrations, Shear test data reduction was first performed with lower order aberrations with astigmatism being removed. The input is shown in Fig. 6. The repeatability of the measurement is  $\sim 10\text{nm}$ . By mechanical control and measurement, we know the mirror position to  $\sim 1\text{mm}$ .

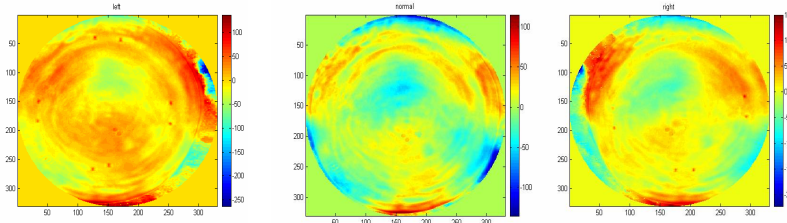


Fig.6. Shear interferograms of the NST test

A total 231 terms of Zernike polynomials were used to describe each surface in MLE. Estimate results are shown in Fig.7. The estimate of the mirror figure was  $\sim 21\text{nm}$ , while the estimate of the test optics was  $\sim 15\text{nm}$ , and we also have 13nm errors in the null space.

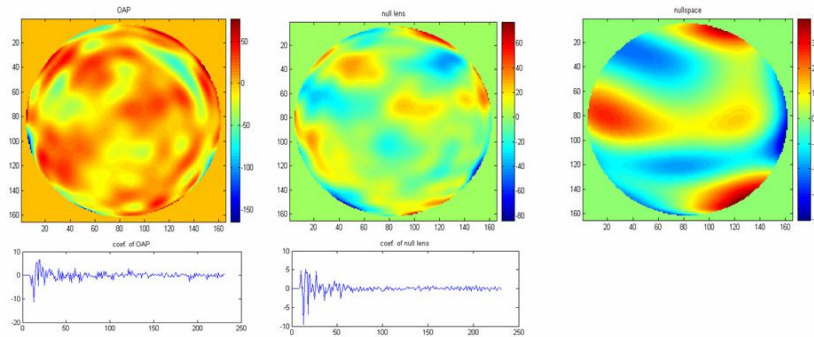


Fig.7. Estimate results

With 231 terms of Zernike polynomials, we could not fully describe the data. We lost approximately 11nm of higher order data information in each interferograms as shown in Fig. 8.

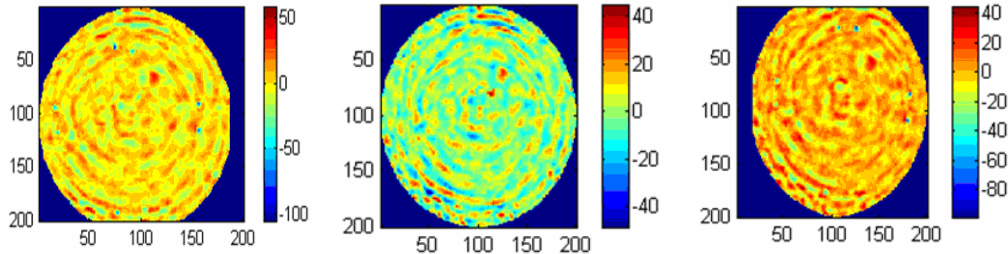


Fig.8. Basis error

We also had approximately 6 nm analysis residuals, which were the fitting residuals from the data described by 231 terms. They reflected the consistency between the model and the measurement data.

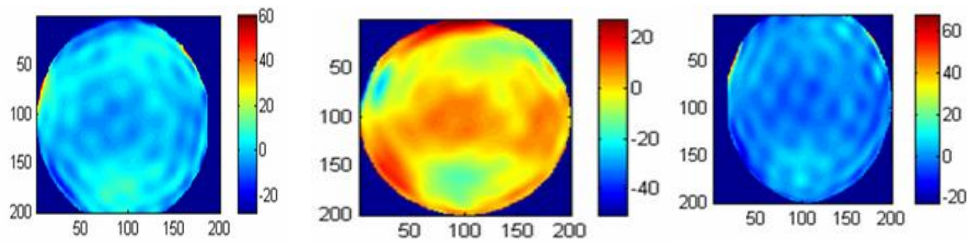


Fig.9. Fitting error

Subtracting the estimated test optics error from the phase data, we had an estimate of the mirror rising from 24nm to 28 nm.

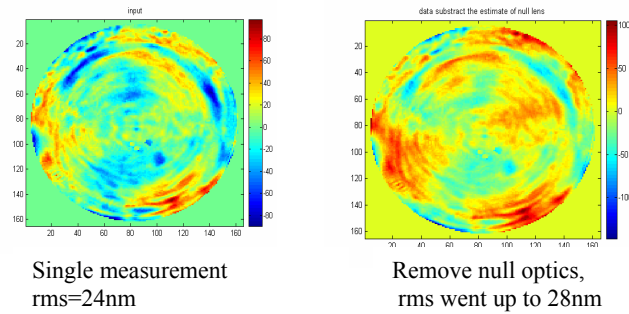


Fig.10. Single measurements and result after correcting null optics error

### 3.2 Estimate surfaces considering lower order aberrations

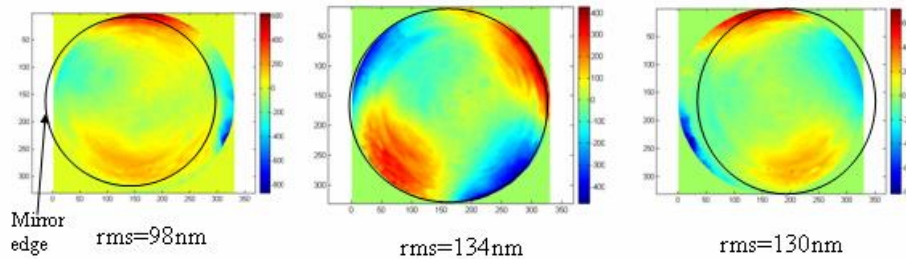


Fig.11. Shear interferograms of the NST test with lower order aberration included

Three sets of data containing lower order aberration shown in Fig.11 were used as input to the MLE. Fig. 12 shows the estimate results. In comparing coma was shown to be zero in normal position measurement after removing the alignment errors, the shear test told us that there were was quite a large amount of coma in the null optics and the mirror. This is consistency with a recent penta-prism test measurement result [5]. However, because we had relative large measurement uncertainties in lower order aberrations, we obtained about 25 nm analysis residuals, which reflected the inconsistency between the measurement data. This could be the real surface shape changing due to the change of the support between the measurements.

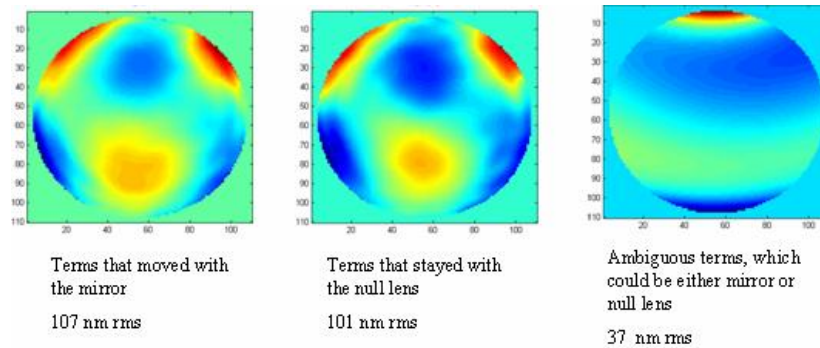


Fig.12. Estimate result considering lower order aberrations

#### 4. DISCUSSION

We have described a shear test that can be used to separate errors in the test optics from errors in the surface under test. Our novel methodology uses Winner filterers, SVD, MLE, and least squares techniques for data processing. Data noise has also been considered in our analysis. Several issues need to be further considered. For example, when a mirror is large, surface distortion resulting from the support change needs to be calculated and subtracted from the measured figure change. To describe the higher order data in the surfaces, a large number of polynomials need to be used. A better set of basis functions is worth investigation.

In all, this shear test has the advantages of ease of implementation and low cost. It is especially good at detecting high frequency information, low order errors with large magnitude and local edge effects of the mirror. The MLE data reduction method can be used as a general way of reducing the data from a shear test of off-axis surfaces.

#### 5. ACKNOWLEDGEMENT

We would like to thank Chunyu Zhao and Brian Smith at the University of Arizona for testing help.

#### REFERENCES

1. R. E. Parks, "Removal of test optics errors," in *Advances in Optical Metrology*, N. Balasubramanian and J. C. Wyant, eds., Proc. SPIE **153**, 56–63 (1978).
2. J. H. Burge, L.B.Kot, H.M.Martin, C.Zhao, T. Zobrist, "Alternate surface measurements for GMT primary mirror segments", Proc. SPIE **6273**, 62732T (2006)
3. William Press, Brian Flannery, Saul Teukolsky, William Vetterling, "Numerical recipes: the art of scientific computing", Cambridge University Press (1986).
4. Peng Su, J.H. Burge, R. Sprowl, J. Sasian, "Maximum Likelihood Estimation as a General Method of Combining Sub-Aperture Data for Interferometric Testing," in *International Optical Design Conference 2006*, Proc. SPIE 6342 (2006).
5. Peng Su, J.H. Burge, Jose sasian, " a pentaprism test of an off-axis parabola", in processing.